Dynamics of Reactive Polymer Networks in the Presence of a Nonpolar Solvent by Dielectric Relaxation Spectroscopy

Saša Andjelić and Jovan Mijović*

Department of Chemical Engineering, Chemistry and Materials Science, Polytechnic University, Six Metrotech Center, Brooklyn, New York 11201

Received December 23, 1997; Revised Manuscript Received March 2, 1998

ABSTRACT: An investigation was carried out on the dynamics of polymer networks in the presence of a nonpolar solvent. The formulations studied were composed of a network-forming multifunctional epoxy−amine mixture and *o*-terphenyl as solvent. A number of formulations at various degrees of cross-linking and with different solvent concentration were prepared and investigated. Experimental results were generated by simultaneous broad-band dielectric relaxation spectroscopy and remote fiber-optic Fourier transform infrared spectroscopy. The emergence of specific interactions during the network formation was confirmed by FTIR and their effect on the dynamics of the α process was established. Dielectric data were analyzed in the time and frequency domain, and it was found that the network dynamics could be classified into three regimes as a function of degree of cure. The nature of relaxations in these three regimes was discussed. An interesting finding was that the dynamics were dominated by the short-range interactions in the vicinity of the gel point. The presence of solvent had a pronounced effect on the various aspects of dynamics, including the apparent activation energy for the α process, the distribution function, and the cooperative nature of relaxations.

Introduction

The use of broad-band dielectric relaxation spectroscopy (DRS) to study dipole dynamics in the glass-forming reactive polymer networks has been recently reported by several groups.[1−4] A chronological evolution of the research on this subject, complete with pertinent references, has been described in a recent communication from our group,[5] while the readers interested in an extensive up-to-date overview of DRS should consult the excellent article by Williams.[6]

Current research efforts (e.g., refs 1−4) are aimed at understanding how the progress of chemical reactions in network-forming polymers affects the dynamics of two major relaxation processes in the frequency domain, namely α and β. This is being accomplished by using broad-band DRS to monitor and analyze the characteristic relaxation times of α and β processes, their temperature dependencies, activation energies, and the breadths and shapes of their distribution function at the various stages of network formation. The experimental strategy is generally 2-fold. Dielectric data in the frequency domain are collected by performing (1) frequency sweeps at selected times during an isothermal reaction and/or (2) frequency sweeps on partially cured samples at selected temperatures where no chemical reactions take place. Fournier et al.[1] studied molecular dynamics during the bulk polymerization of an epoxy−amine formulation by combining the results of DRS and differential scanning calorimetry (DSC) in an effort to understand how dielectric data can give information on the kinetic changes that lead to glass formation. The measured changes in dynamics and kinetics during cure were correlated and a model has been developed that allows DRS to predict the course of the reaction in the vitrification range. One important conclusion from their work is that the reactions become diffusion controlled at times when the dielectric loss described by $\epsilon''(t,f,L,T)$ reaches its maximum value ϵ''_{max} at measurement frequencies below 1 Hz. Casalini et al.[2,3] studied the relaxation of an epoxy−amine formulation during polymerization. The most probable relaxation time for α and β process was described by the Vogel−Fulcher and Arrhenius equations, respectively, and the description of each relaxation process included the dependence of relaxation time on both temperature *and* conversion. They also reported a linear increase in the activation energy of the β process with conversion. Our recent studies of the reorientational dynamics of dipoles during the network formation in multifunctional epoxy−amine formulations had an additional dimension in that the results were generated by simultaneous DRS and Fourier transform infrared (FTIR) spectroscopy.[4] We described the molecular origin of a relaxation, proposed a methodology for the evaluation of the kinetics of network formation, and advanced an interpretation of the network dynamics in terms of intermolecular cooperativity based on the interplay between molecular and dielectric architecture. The ability to generate FTIR and dielectric spectra simultaneously proved to be of the utmost importance.

In this communication we address a related issue which, surprisingly, has been largely unexplored in the literature. Of interest here is to examine the effect of the addition (at various concentrations) of a nonpolar, nonreactive solvent on the dynamics of the growing polymer network. There are numerous important questions one should ask. Does the presence of a nonpolar solvent alter the various specific interactions observed in the neat (solventless) system at various stages of cure? Do dipoles on solute molecules relax in a cooperative motion with the solvent? What is the underlying mechanism by which solvent alters the network dynamics? In this study we have sought to answer these questions by investigating an epoxy−amine network during cure in the presence of *o*-terphenyl (OTP)—a compatible, high molecular weight, high boiling point,

* To whom correspondence should be addressed.

S0024-9297(97)01851-2 CCC: $15.00
Published on Web 04/08/1998

nonreactive, nonpolar, glass-forming solvent. Interactions in nonpolar solvent/solute mixtures have been investigated by DRS (e.g., ref 7 and references therein), although the vast majority of such studies have examined binary mixtures of low molecular weight compounds and, to the best of our knowledge, none considered a reactive network-forming solute. Nonetheless, some of the reported studies are of particular importance because of their direct relevance to our work and should be singled out. For instance, a series of studies of DRS of the supercooled solutions of nonreactive solutes in OTP have been conducted by Williams and co-workers,[8−11] and in some sense we have built upon their work. These authors considered a variety of low molecular weight solutes and found that dipolar molecules in supercooled liquids moved cooperatively with the solvent environment. An interesting aspect of their studies was the use of apparent activation energy as the indicator of the cooperative nature of relaxations. They found that the activation energy was independent of the OTP concentration for some polar solutes, while in others it increased significantly. The physical interpretation of their findings (strangely overlooked in the literature) deserves particular consideration because of the originality and the ability to capture the essential feature of cooperativity in glass-forming substances—currently one of the most widely studied and debated areas of polymer physics. They start by considering a low viscosity liquid and assume that the reorientation of the reference dipole takes place within a spherical shell which contains within it all molecules that make an important contribution to the average dipole moment correlation function. As the temperature is lowered, the kinetic energy and entropy of the molecules decrease, leading to an increase in the size of the cooperative sphere around the reference molecule. At sufficiently low temperatures the sphere may encompass hundreds of molecules which reorient as if they were "enmeshing cogs". The students of dynamics of glass-forming materials will immediately recognize that this concept predates and defines the basis for a number of subsequently proposed models for cooperative motions and length scales in glass-forming substances (e.g., refs 12−14),

An important consideration in this work regards the miscibility of our epoxy−amine formulation and OTP over a wide range of conversion, because of the potential effect of phase separation on the measured dielectric response. We found no such information in the literature, though several authors have considered a related issue of the OTP morphology. For example, structural irregularities of OTP molecules of the nanoscale size were invoked by McLaughlin and Ubbelohde,[15] who postulated the formation of clusters composed of several OTP molecules above the melting point and in the supercooled state. Higashigaki and Wang[16] claimed that such clusters could not form in liquid OTP, despite the fact that their Rayleigh−Brillouin scattering studies revealed a long-lived translational structure in the supercooled liquid. Cicerone and Ediger[17] used time-resolved optical spectroscopy to analyze the dynamics of different probe molecules in the supercooled OTP and reported a spatially heterogeneous behavior at nanoscale levels. In our case, however, all formulations are transparent at any time during cure, suggesting the absence of microphase separation (the presence of nanoscale clusters of OTP is still possible) that would have an effect on the measured dielectric response. We shall return to this subject later in the text.

The principal objective of this communication is to examine how the advancement of chemical reactions affects the dynamics and cooperativity in polymer-forming networks in the presence of a nonpolar, nonreactive solvent. To the best of our knowledge this communication marks the first time that the dynamics of thermoset polymer networks at various stages of cure have been investigated in the presence of solvent.

Experimental Section

Materials. The formulation studied was composed of the diglycidyl ether of Bisphenol A, or DGEBA (Epon 825, Shell Chemical Company), 4,4′-methylenedianiline, or MDA, (Ciba-Geigy XU HY 205), and *o*-terphenyl, or OTP (Aldrich). Stoichiometric amounts of the epoxy group and the amine hydrogen were used, and tests were performed at different frequencies, times, and temperatures. The various formulations are defined throughout the text by the general form *X*/*Y*, where *X* represents the weight percentage of the solute (i.e., a DGEBA−MDA mixture) and *Y* represents the weight percentage of the solvent (OTP). For example, a 33/67 formulation is composed of 33 wt % of a stoichiometric DGEBA−MDA mixture and 67 wt % of *o*-terphenyl.

Techniques. (A) Dielectric Spectroscopy. Our experimental facility for dielectric measurements consists of modified commercial and custom-made (in-house) instruments and has been described in detail elsewhere.[5] Parts of the data analysis were performed with Novocontrol System's WinFit software (courtesy of Dr. Gerhard Schaumburg).

(B) Infrared Spectroscopy. Fourier transform infrared (FTIR) spectroscopy was performed simultaneously with dielectric measurements in a setup described elsewhere.[4]

(C) Differential Scanning Calorimetry. Some supporting evidence was obtained from DSC using TA Instrument Co. DSC model 2920 at a heating rate of 10° C/min.

Results and Discussion

Near-Infrared (NIR) Fourier Transform Spectroscopy. We begin our discussion by presenting the results of NIR spectroscopy for several solvent-containing formulations at various degrees of cure. It was anticipated that NIR spectra would shed light on the chemical and physical phenomena that accompany network formation by identifying the type and concentration of different chemical groups at various stages of cure, the interactions between them and the reaction kinetics. In Figures 1 and 2 we show a series of spectra obtained during cure of 33/67 and 50/50 formulations at 120 and 140 °C, respectively. The progressive changes in the spectra were systematic and conducive to a precise quantitative analysis. The trends displayed by the major peaks of relevance in the epoxy/amine reactions were evident; a decrease in epoxy absorption (4530 and 6080 cm^{-1}), a decrease in primary amine (5060 cm^{-1}) and primary and secondary amine absorptions (6670 cm^{-1}), and an increase in hydroxyl absorption (7000 cm^{-1}). The absence of an absorption peak at 5240 cm^{-1} confirmed that both systems were free of any significant amount of absorbed moisture. A comprehensive account of the origin, locations, and shifts of all NIR peaks during epoxy/amine reactions is given elsewhere.[18]

Spectral data of the type shown in Figures 1 and 2 were used to determine the reaction kinetics, according to the methodology documented in the literature.[19,20] The extent of reaction (α) at any time (t) is calculated from the initial areas of epoxy and reference peaks,

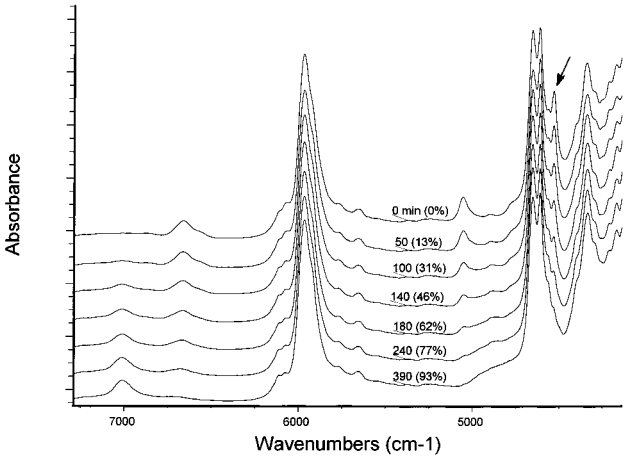

Figure 1. NIR spectra during isothermal cure of 33/67 formulation at 140 °C at different reaction times (in minutes). Percent conversion is given in parentheses. The arrow indicates the epoxy peak used for kinetic studies.

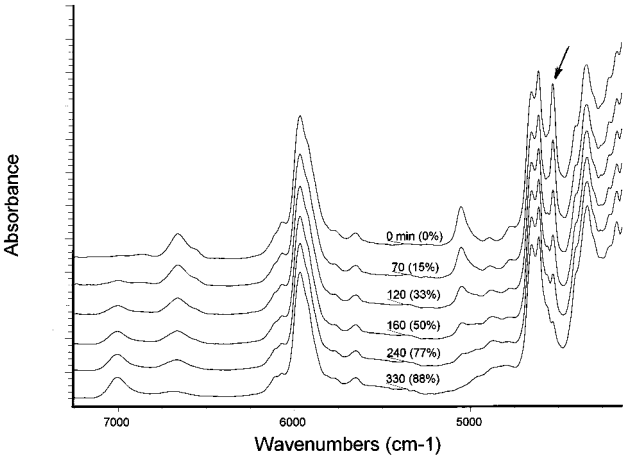

Figure 2. NIR spectra during isothermal cure of 50/50 formulation at 120 °C at different reaction times (in minutes). Percent conversion is given in parentheses. The arrow indicates the epoxy peak used for kinetic studies.

$A_{epoxy}(0)$ and $A_{ref}(0)$ respectively, and their corresponding values at time t, $A_{epoxy}(t)$ and $A_{ref}(t)$ with the following equation:

$$\alpha = 1 - [(A_{epoxy}(t))(A_{ref}(0))]/[(A_{epoxy}(0))(A_{ref}(t))] \quad (1)$$

In this study, the peak at 4530 cm^{-1} was utilized to monitor the disappearance of the epoxy group. The primary amine kinetics were evaluated using the area under the peak at 5060 cm^{-1}. Benzene absorption at 4620 cm^{-1} was employed as a reference peak. Figure 3 affords a comparison of the kinetic results for 100/0 (neat), 50/50, and 33/67 formulations at different reaction temperatures. An increase in the OTP concentration results in a decrease in the reaction rate, and higher temperatures are needed to complete the cure. For instance, the neat formulation at 84 °C reacts much faster than the two solvent-containing formulations at higher temperature, while 33/67 formulation at 130 °C reacts considerably slower that 50/50 formulation at 120 °C. The information contained in Figure 3 was used to prepare samples of a precisely known degree of cure.

Spectroscopic evidence did not reveal a change in the reaction mechanism in the presence of solvent, and no further attempts at deriving mechanistic kinetic equations were made: we focused our attention on network dynamics instead of reaction kinetics. However, NIR spectroscopy revealed two types of specific interactions that directly affect the dynamics and as such were investigated in greater detail. These are (1) specific interactions which form between polar groups immediately upon mixing of the ingredients (epoxy and amine) and which persist up to about 10% conversion and (2) specific interactions owing to the hydrogen-bonded complexes that form as a network approaches the gel point.[4] We will now briefly describe the first type of these interactions and will address the question of hydrogen-bonded complexes later in the text in conjunction with the dielectric response near the gel point.

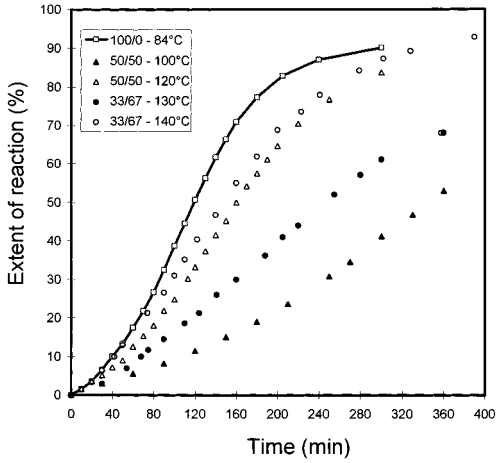

Figure 3. Extent of reaction as a function of reaction time. A comparison of the results for 100/0 (neat), 50/50 and 33/67 formulation at different reaction temperatures.

In our previous study of the neat formulation[4] we used NIR results to argue the emergence of dipole−dipole interactions in the as-mixed nonreacted formulations. Initially, these interactions impose conformational restrictions to the mobility of dielectrically active species and affect dynamics but are gradually relaxed as the cure progresses. The presence of specific interactions in the neat nonreacted formulation is manifested in the NIR spectra by an *increase* in the absorption intensity of moieties (epoxy, amine) that partake in these interactions with *increasing* temperature. At the same time, the absorption intensities of the moieties (benzene rings, methylene groups) that do not engage in specific interactions follow a characteristic *decreasing* trend with *increasing* temperature. In the solvent-containing formulations, however, this effect is gradually reduced with an increase in solvent concentration, and it disappears in formulations with over 70% OTP.

Another interesting finding is the unusual *increase* in the intensity of amine absorption peaks observed during the first 10% conversion in all isothermal nonpolymer-forming and polymer-forming epoxy−amine mixtures. Above 10% conversion, however, this trend is reversed and we observe a *decrease* in the amine absorption intensity that mimics that of the epoxy group. We have previously reported[21] a detailed kinetic study of a model system composed of phenylglycidyl ether and *N*-methylaniline. We monitored the various NIR amine absorption peaks and found out that during the first 10% conversion the stretching vibration intensity (6700 cm^{-1}) increased considerably, while the combination band intensity (5000 cm^{-1}) decreased at a

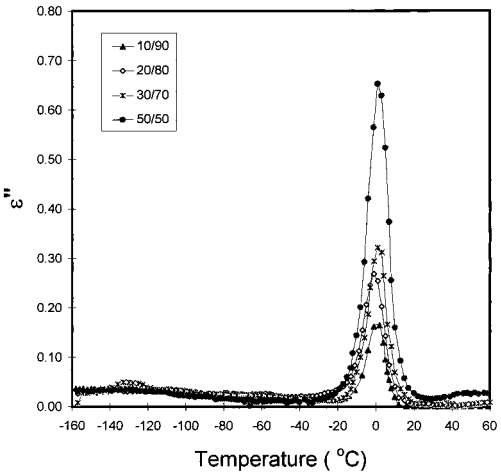

Figure 4. Dielectric loss as a function of temperature at 25 kHz with composition as a parameter for four nonreacted formulations.

rate equivalent to that of the epoxy group. Above that "critical" conversion stage (10%), however, the stretching vibrational intensity decreases at the same rate as those for other reactive groups. A generalized explanation for this seemingly anomalous behavior can be offered in terms of the formation of strong dipole−dipole interactions between functional groups in the initial mixture. The fact that certain vibrational modes (i.e., the above cited stretching mode in a secondary amine) are "frozen in" in the initial mixture, but become active as the reaction progresses, suggests the existence of a high-energy conformation. We envision the vibrational motions of dipoles on functional groups as being impeded by restrictions that could be, in general, unidirectional, whereby stretching modes are affected, and/or multidirectional, whereby bending and/or combination modes are affected. In either case, however, these restrictions are gradually relaxed with the advancement of cure. A reaction product formed by the collision of two functional groups is a bigger and stiffer molecule and as such helps diminish the restrictions to vibrational motions of dipoles on neighboring molecules by excluding them, physically, from its sphere of influence. The net result is a decrease in dipole−dipole interactions. Since the same dipoles involved in specific interactions are at the heart of relaxation processes measured by DRS, it is expected that these conformational restrictions should have an effect on the dynamics. We shall see later in the text that this is indeed the case.

Dielectric Relaxation Spectroscopy (DRS). In this section we present the results of dielectric measurements on a series of formulations at various stages of network formation and with different solvent concentration. Dielectric measurements were performed almost exclusively in the frequency domain with temperature as a parameter. Several approaches to describing the dynamics of these networks have been explored and are discussed below.

A. Nonreacted System. We first examined a series of nonreacted (0% conversion) formulations with varying OTP concentration. Figure 4 shows the dielectric loss as a function of temperature for four nonreacted formulations of different composition. The scans were performed at a constant frequency of 25 kHz, and several interesting features are readily noticed. A pronounced a relaxation is found in all samples; it is centered around 0 °C, and its intensity systematically

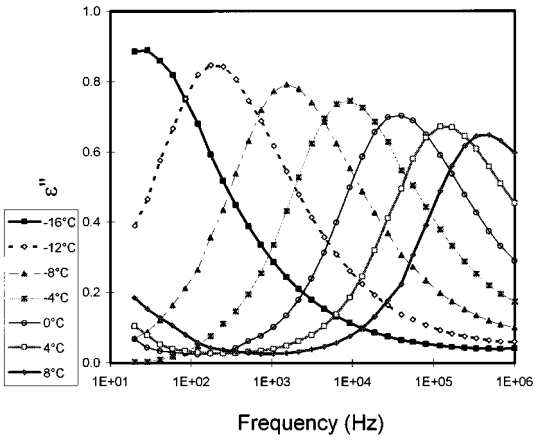

Figure 5. Dielectric loss in the frequency domain with temperature as a parameter for a nonreacted 50/50 formulation.

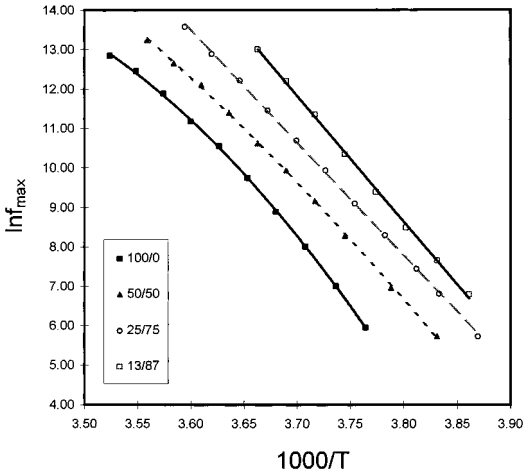

Figure 6. The ln frequency at dielectric loss maximum (f_{max}) vs $1/T$ for nonreactive 100/0 (neat), 50/50, 25/75, and 13/87 formulations. Data are shifted horizontally for clarity.

decreases with an increase in the OTP concentration. The peak intensity was estimated as the product of its width and its height in the frequency domain. The calorimetric glass transitions (measured by DSC) of OTP and the nonreacted DGEBA/MDA mixture are very close, −23 and −19 °C, respectively, and hence one would not anticipate a shift in the location of the dielectric loss peak along the temperature scale as a function of the OTP concentration. However, since the contribution of OTP to the measured dielectric loss is assumed to be negligible,[10] it is clear that the peak intensity must decrease with a decrease in the amount of DGEBA/MDA in the formulation. One consequence of this is that the secondary relaxations, which were observed in the neat formulation, are progressively more difficult to detect in the OTP-rich formulations.

Dielectric loss in the frequency domain with temperature as a parameter for the nonreacted 50/50 formulation is given in Figure 5. The corresponding activation energy was determined by plotting the logarithm of frequency at maximum loss (f_{max}) as a function of reciprocal temperature, as shown in Figure 6. The calculated apparent activation energies for several solvent containing formulations were in the range of 240−260 kJ/mol. At this point we recall the above-described specific interactions that form in the early stage of cure and show how these interactions affect dielectric response. In contrast to a strong non-Arrhe-

Table 1. Power Law Exponents "*m*" and "*n*", Activation Energy, and the Increase of the Half-Bandwidth of Normalized Relaxation Peak for 50/50 Formulation During Cure

extent of reaction calculated by NIR (%)	*m*	1 − *n*	E_a (kJ/mol)	E_a (kcal/mol)	half-band width increase (%)
0	0.73	0.48	243	57.8	0
10	0.75	0.51	244	58.2	−1.8
20	0.66	0.49	239	56.8	+4.2
33	0.49	0.46	227	54.1	23.4
40	0.425	0.42	223	53.0	42.6
50	0.34	0.35	217	51.7	72.3
55	0.28	0.30	216	51.5	106
60	0.275	0.19	299	71.0	185
65	0.25	0.19	330	78.7	193
70	0.215	0.19	322	76.7	206
80	0.205	0.15	277	66.0	232

nius behavior observed for the neat formulation (included in Figure 6 for completeness), the relaxation behavior of all solvent-containing formulations used in this study could be approximated by the Arrhenius form in a frequency range between 100 Hz and 1 MHz. When the OTP content is increased in a formulation, we observe a gradual decrease in the curvature of the apparent activation energy map, as a result of the weakening of dipole−dipole interactions and a simultaneous decrease in cooperativity. Formulations containing more than 70% OTP show a distinct Arrhenius behavior in the same frequency range. We envision the role of OTP molecules as one of separating the dipoles and thereby reducing the dipole−dipole interactions. We emphasize here that dielectric and NIR data led to the same conclusion, and hence both techniques could be used to probe specific interactions present in the initial stage of epoxy−amine cure.

B. Partially Reacted Systems. The next step was to investigate the dynamics of partially cured solvent-containing samples. In general, the solvent-containing formulations differed from the neat formulation in the following ways: (1) a slower increase in the glass transition (DSC) during cure; (2) little or no trace of ionic conductivity found in the frequency window of our dielectric measurements; (3) a lack of correlation between the half-width of the normalized dielectric loss peak and the extent of reaction calculated from the NIR spectra (see Table 1). On the other hand, all solvent-containing formulations resembled the neat formulation in that the dielectric loss peak at 100% conversion was completely suppressed. The question of miscibility of the epoxy−amine formulations and OTP has been brought up in the Introduction and is briefly revisited below. We observed completely clear, transparent samples at any time and/or stage of reaction for all DGEBA−MDA/OTP formulations studied. Further, DSC measurements revealed the existence of a single glass transition in a 50/50 formulation throughout the entire cure cycle. It should be noted, however, that in the later stages of cure in solvent rich formulations (e.g. 33/67) we observed two glass transitions: one due to the miscible DGEBA−MDA/OTP phase and the other, located at around −25 °C, due to OTP. However, this separate domain of OTP molecules is not engaged in the polymer network dynamic and hence does not influence the dielectric response.

C. Activation Energy. In Figure 7we show an example of dielectric loss peak in the frequency domain with temperature as a parameter for a 50/50 formulation at 55% conversion (based upon the consumption of epoxy groups). As expected, the α relaxation *loss peak maximum* shifts to a higher frequency with increasing temperature. The *loss peak intensity*, on the other hand, shows a peculiar trend. In nonreacted samples, the loss intensity *decreases* with increasing temperature, but as the cure progresses, this trend is gradually reversed and eventually the loss intensity begins to *increase* with increasing temperature (see Figure 5). This is particularly intriguing when one considers that thermodielectric simplicity (described in the following section) is preserved up to 70% conversion. This phenomenon is not observed in a neat DGEBA−MDA mixture and is caused by the OTP molecules, though its exact mechanism remains unclear at present. Data from the frequency sweeps were used to generate the plots of the logarithm of frequency at loss peak (f_{max}) as a function of reciprocal temperature for a number of formulations at various stages of network formation and with different OTP concentration. An example of one such plot is shown in Figure 8. It is clear from this figure that the formation of the network inhibits the rate of motion of active dipoles. The activation energy for a 50/50 formulation at different conversion was determined from the linear portion of the relaxation map between 100 Hz and 1 MHz, and the calculated values are sum-

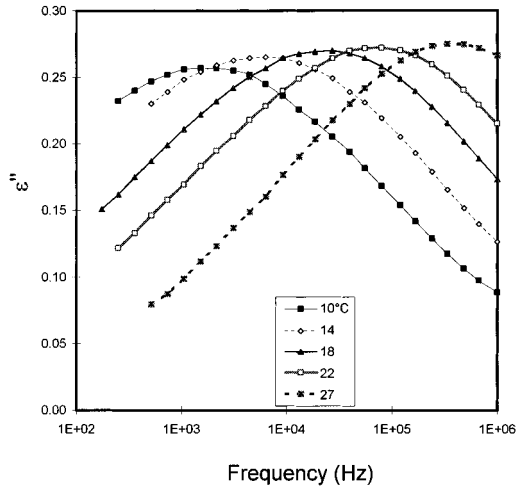

Figure 7. Dielectric loss in the frequency domain with temperature as a parameter for a 50/50 formulation at 55% conversion.

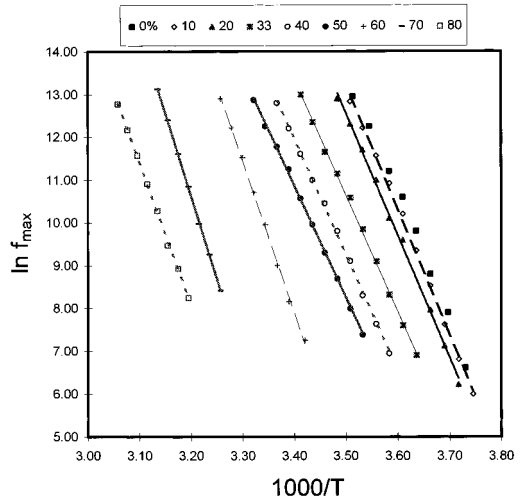

Figure 8. The ln frequency at dielectric loss maximum (f_{max}) vs 1/*T* for a 50/50 formulation at various degrees of cure.

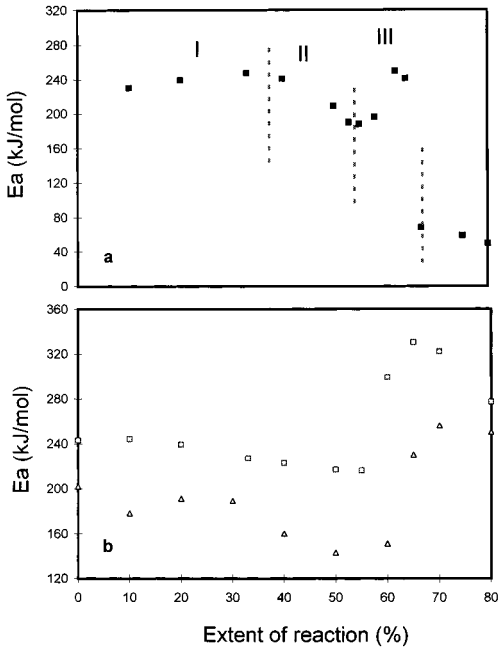

Figure 9. Activation energy vs extent of reaction for (a) the 100/0 (neat) formulation and (b) 50/50 and 33/67 formulations. Zones I, II, and III indicated on the plot are described in the text.

marized in Table 1. The question of how and why the activation energy varies as a function of degree of cross-linking in the network is addressed next. In Figure 9b we plot the activation energy for 33/67 and 50/50 formulations as a function of extent of reaction. The overall trend in the activation energy for these two formulations during cure is almost identical, the only difference being that the data for the 33/67 formulation are shifted downward. Moreover, this trend is generally in good agreement with that observed for the neat formulation, included for completeness in Figure 9a. The change in the activation energy during cure for all formulations can be conveniently described by dividing the observed response into three regimes, labeled I, II, and III and separated by dashed lines (Figure 9a,b). In regime I, which extends to approximately 35% cure, the dominant reaction in the mixture is between epoxy and primary amine groups, and the principal product is a linear chain of a continuously increasing molecular weight. Above approximately 35% we enter regime II, where secondary amine−epoxy reactions become important and a cross-linked network begins to form. Dipoles that contribute primarily to the α process (terminal epoxy and to some extent primary amine) continue to be replaced by less dielectrically active secondary and tertiary amine and hydroxyl groups, resulting in a decrease in the interactions between the epoxy and other dipoles and, consequently, the lowering of the activation energy (and cooperativity, as will be shown later) for the α process. We have termed this phenomenon "dipole dilution effect"[4] and submit that it represents an inherent characteristic of the network forming epoxy−amine formulations. Most interestingly, however, the activation energy reverses its decreasing trend at about 55% cure; it increases until approximately 62% conversion, and then it decreases again. There are two important points here. First, this trend is observed in all formulations, with or without solvent. And second, this peculiar change in the activation energy is observed in the vicinity of the gel point, which

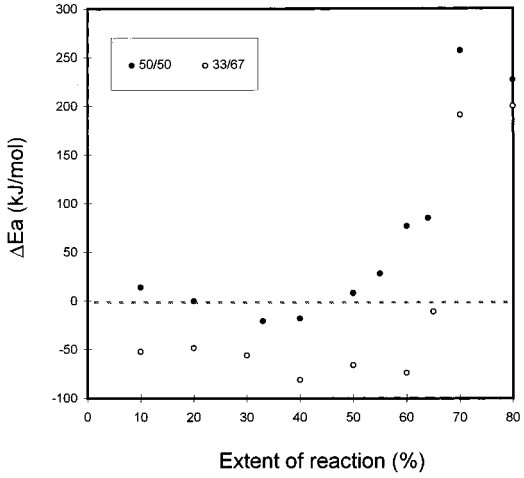

Figure 10. Difference (ΔE_a) between the activation energy of a solvent-containing formulation (50/50 and 33/67), and that of the neat formulation (100/0).

occurs at about 60% (determined by IR spectroscopy) in this system. This observed behavior is caused by an interplay of the physical and chemical changes on the molecular level that set in as the network approaches the gel point. The physical change in the network is manifested as a decrease in the distance (densification) between the polar groups in the reactive mixture, whereas the chemical change is associated with the formation of specific hydrogen-bonded complexes. The emergence of these complexes is contingent upon reaching a critical combined concentration of epoxy, amine, and hydroxyl groups; the nature of these complexes has been discussed in more detail elsewhere,[4,22] and only the salient features of this concept are recapped below. Once formed, these complexes increase the steric hindrance and the intermolecular rigidity of the network, while at the same time impeding the reorientational motions of terminal epoxy groups (which are at the heart of the α process). That, in turn, leads to the creation of a higher activation energy state. However, the lifetimes of these complexes are short and confined to a narrow conversion range since the advancement of cure leads to the depletion of epoxy and secondary amine groups and a subsequent break-up of the conditions for the existence of a critical concentration of different moieties in the mixture. At that point the activation energy begins to decrease and that is where we see a major difference between neat and solvent-containing formulations. In the neat formulation the activation energy drops to about one-fifth of its initial value at about 70% conversion, while the drop in the solvent-containing formulations is much less pronounced. The higher activation energy in the latter stages of cure in solvent-containing formulations suggests that solvent molecules directly affect the reorientational dynamics of the epoxy network. A further insight into this phenomenon can be obtained by plotting the difference (ΔE_a) between the activation energy of a solvent-containing formulation and that of the neat formulation, as shown in Figure 10. The dashed line should be viewed as a reference along which there is no difference between the activation energy of neat and solvent-containing formulations; a large discrepancy between the activation energy of the neat formulation and either of the two solvent-containing formulations observed in the later stages of cure (i.e. large ΔE_a in Figure 10), indicates a strong effect of the solvent. We interpret

the results of Figure 10 to mean that the restrictive effect of the solvent on the dynamics of our epoxy−amine networks increases considerably as the gel point is approached and persists from there on. The physical basis for this phenomenon is considered below.

D. Breadth and Shape of the Relaxation Spectrum. D.1. Relaxation in the Time Domain. We proceed to describe the dynamics of the α process by fitting the normalized dielectric loss data (for networks at various conversions) to the Kohlrausch−Williams−Watts (KWW), or stretched exponential expression.[23] This procedure has been described and utilized in our earlier study of the neat formulation,[4] where we found that the KWW parameter β was linearly proportional to the degree of cure and that it could therefore be used to correlate dipole dynamics with the kinetics of network formation. In general, however, this was not possible in the solvent-containing formulations, where only the initial nonreactive mixture and a 10% cured sample yielded good KWW fits with $\beta = 0.52$ and 0.53, respectively. Above 10%, however, no fits to a stretched exponential were possible. Characteristic examples are shown in Figure 11a−d, which contain normalized loss curves and the corresponding KWW fits for various formulations cured to between 10 and 70% conversion. Although the normalized loss data are superposable (i.e. are thermodielectrically simple), Figure 11a−d shows that a stretched exponential cannot fit the data adequately. Since the β process falls outside the frequency window of Figure 11a−d, it is clear that OTP exerts an influence on the shape of the a relaxation throughout (practically) the entire cure process.

D.2. Relaxation in the Frequency Domain. Jonscher's power law approach and the Havriliak−Negami equation were used to describe the α process in the frequency domain. The basic tenet of Jonscher's concept[24] is that the frequency dependence of the dielectric loss peak could be universally represented by two power laws combined in the following equation:

$$\epsilon''(\omega) \propto 1/[(\omega/\omega_p)^{-m} + (\omega/\omega_p)^{1-n}] \qquad (2)$$

Here ϵ'' is the dielectric loss, ω_p is the peak frequency, and m and n are the power law exponents that fall in the range between 0 and 1. Exponents "m" and "n", calculated at various stages of cure, are listed in Table 1. Jonsher[24] and Dissado and Hill[25] have argued that "m" and "n" represent two separate and independent molecular processes which led Schönhals and Schlösser[26] to propose a physical picture that relates "m" to a large scale molecular mobility and "n" to the local chain motions. They studied the shape parameters of dielectric relaxation of cross-linked polyurethanes and suggested a methodology to relate them to small and large scale molecular interactions. In parts a and b of Figure 12 we plot "m" and "n" for a 50/50 formulation and a neat formulation, respectively, as a function of extent of reaction. A careful inspection of these figures indicates that the variation in "m" and "n" can be divided into three regimes along the extent of reaction axis. Interestingly, these three regimes, labeled I, II, and III for convenience, correspond closely to the three regimes in the activation energy (described in Figure 9a,b) which were invoked earlier to rationalize the effect of chemical and physical changes that accompany the network formation on dipole dynamics. We now show how a supporting argument to the proposed concept of the molecular length scale of dipole dynamics can be put forward in terms of the changes in "m" and "n". Let us begin by pointing out that both "m" and "n" decrease during cure, reflecting the broadening of the relaxation spectrum. However, how fast these exponents decrease during cure, both individually *and* with respect to one another, are important questions that could shed light, at least qualitatively, about the molecular origin of the relaxation process (assuming that "m" and "n" could indeed be related to the large and small scale motions, respectively). In this context Figure 12 is quite informative. In the first stage of cure, up to 35% conversion (regime I), the principal reaction product is a linear chain of gradually increasing molecular weight, which, in turn, would be expected to have a stronger effect on the long range dynamics. Indeed, this is manifested in both formulations (see Figure 12) as a much more pronounced change in exponent "m" in regime I. In regime II, from about 35% to 55% cure, secondary amine−epoxy reactions become important and a cross-linked network begins to form. This region marks the onset of the "dipole dilution effect", which was invoked earlier to explain a rapid decrease in the activation energy. Both "m" and "n" decrease in this regime at about the same rate, suggesting that the effect of network formation on small and large scale dynamics is of comparable magnitude. Finally, in regime III that extends from about 55% to 70% cure and is characterized by the emergence and the subsequent breakup of the hydrogen-bonded complexes, we observe a different trend. Exponent "m", as shown in Figure 12b, continues to decrease at the same rate as in regime II, while exponent "n", which is related to the short chain dynamics, undergoes a pronounced change in going from regime II to regime III: it decreases abruptly in both neat and solvent-containing formulations. We interpret these changes to signify that the reorientational dynamics of dipoles in the vicinity of gel point (where there is a strong influence of hydrogen-bonded complexes) are mainly affected through the short chain interactions.

Next, we fit our data to the Havriliak−Negami expression—a Debye equation modified by the inclusion of two adjustable parameters,[27] α and β, which is given as

$$\epsilon^*(\omega) = \frac{\epsilon_0 - \epsilon_\infty}{[1 + (i\omega\tau)^\alpha]^\beta} + \epsilon_\infty \qquad (3)$$

where $\epsilon^*(\omega)$ is the frequency dependent dielectric constant, ϵ_0 and ϵ_∞ are its relaxed (low frequency) and unrelaxed (high frequency) limits, ω is the angular frequency and τ is the most probable relaxation time. The adjustable parameters α and β account for the symmetric and asymmetric broadening of the relaxation peak, respectively. It is also readily seen that this equation is a generalization of the Cole−Cole equation, to which it reduces for $\beta = 1$, and a generalization of the Cole−Davidson equation, to which it reduces for $\alpha = 1$. In Figure 13 we show dielectric loss in the frequency domain with temperature as a parameter for a 50/50 formulation at 33% conversion; the symbols are data points and the solid lines represent fits to eq 3.

E. Distribution Function. We next sought to establish how the network growth affects the distribution function for the α process, $G(\tau)$, and its temperature dependence. The complete expression for the distribution function for the Havriliak−Negami equation is

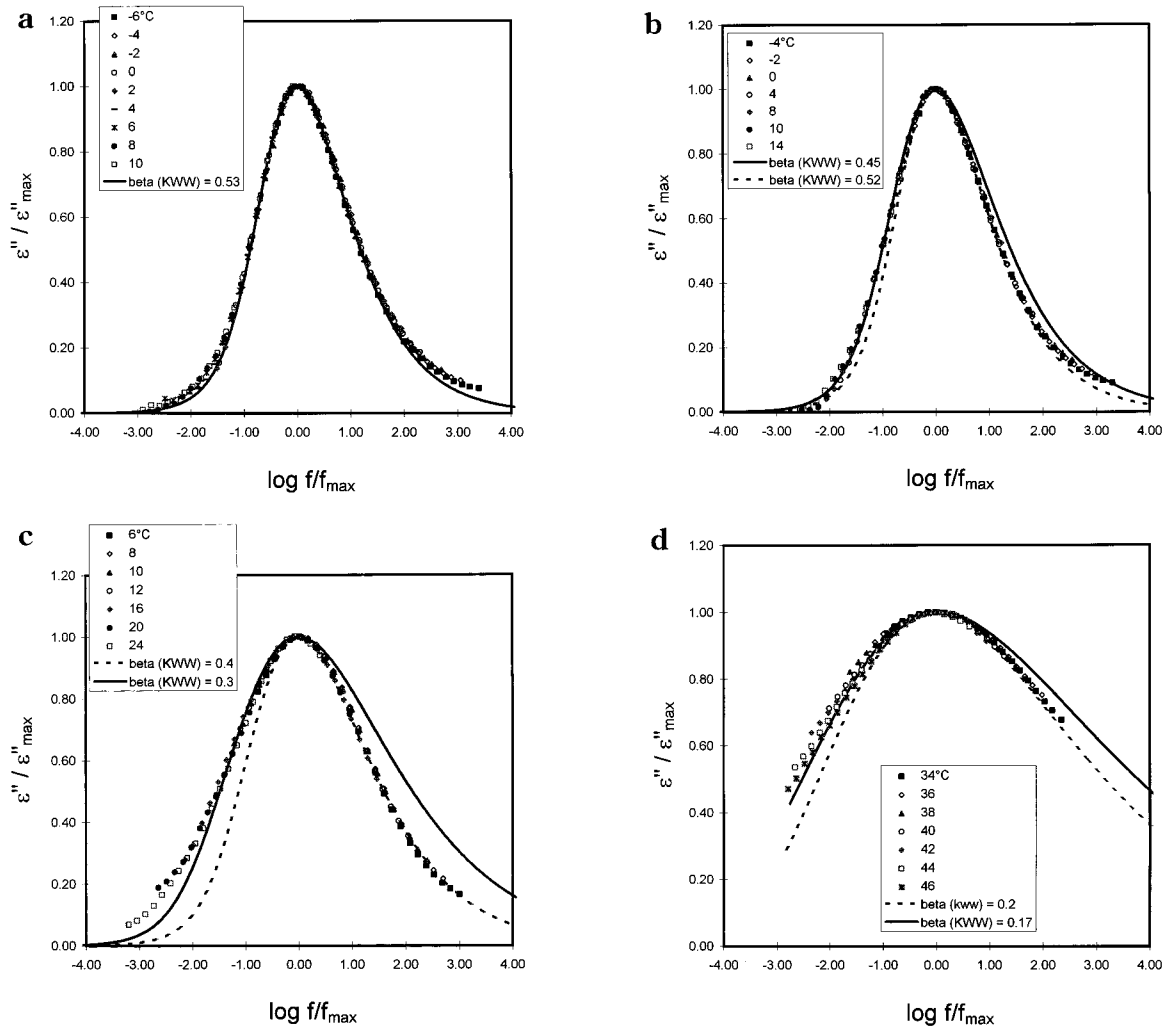

Figure 11. (a) Normalized dielectric loss for 50/50 formulation cured to 10% conversion. A solid line is the fit to the KWW or stretched exponential function. (b) Same as part a for 20% conversion. (c) Same as part a for 40% conversion. (d) Same as part a for 70% conversion.

given as[7]

$$G_i(\tau) = \frac{\left(\frac{\tau}{\tau_{0i}}\right)^{\alpha_i\beta_i} \sin(\beta_i\theta_i)}{\pi\tau\left\{\left(\frac{\tau}{\tau_{0i}}\right)^{2\alpha_i} + 2\left(\frac{\tau}{\tau_{0i}}\right)^{\alpha_i}\cos(\pi\alpha_i) + 1\right\}^{\beta_i(1/2)}} \quad (4)$$

where

$$\theta_i = \arctan\left\{\frac{\sin(\pi\alpha_i)}{\left(\frac{\tau}{\tau_{0i}}\right)^{\alpha_i} + \cos(\pi\alpha_i)}\right\}$$

$$0 \le \theta_i \le \pi$$

The best fit parameters α and β obtained from Figure 13 were inserted into eq 4, and the distribution function was computed for a number of partially cured networks at a series of temperatures. In each case we examined (1) the shape and the breadth of the distribution function and (2) the thermodielectric simplicity (or lack thereof) of the distribution function. To answer these questions we constructed plots of normalized distribution function, $G(\tau)/G(\tau)_{max}$, as a function of normalized relaxation time, τ/τ_{max}. Selected results are displayed in Figure 14a−d for a 50/50 formulation at 10% (Figure

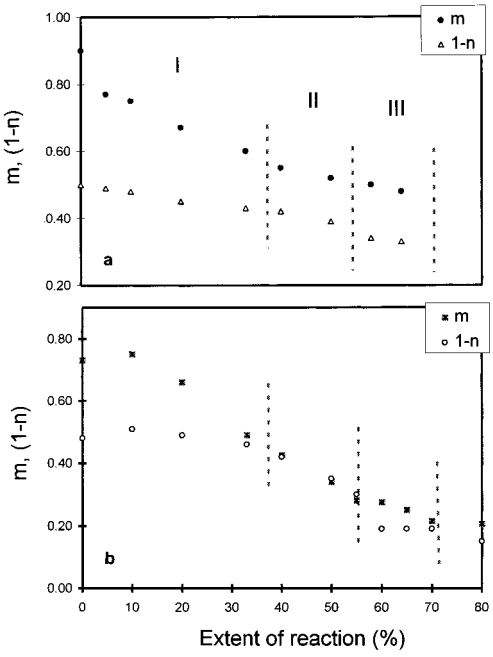

Figure 12. Jonscher's power law exponents "*m*" and "*n*" as a function of extent of reaction for (a) the 100/0 formulation and (b) the 50/50 formulation.

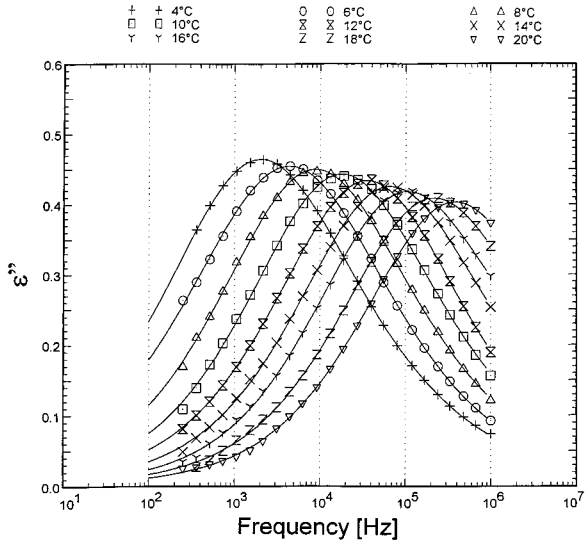

Figure 13. Dielectric loss in the frequency domain with temperature as a parameter for a 50/50 formulation at 33% conversion. The symbols are data points and the solid lines represent fits to the HN equation.

14a), 33% (Figure 14b), 55% (Figure 14c), and 60% (Figure 14d) conversion. First, we would like to discuss the shape and the breadth of the distribution function. The distribution function is initially skewed toward the high frequency end (short relaxation time, see Figure 14a), indicating a broad distribution of short scale motions, but its shape becomes increasingly more symmetric as the cure progresses (see Figure 14b,c). This parallels the observed trend for exponents "*m*" and "*n*" shown in Figure 12b. We stated earlier that up to 35% conversion (regime I), exponent "*n*" undergoes only a slight change with cure, while exponent "*m*" decreases significantly. The implication is that the changes observed at the low frequency end (as defined by the changes in "*m*") of the distribution function dominate the dynamics in this stage of cure. Between approximately 35% and 55% conversion, these two exponents are equal and decrease at the same rate. The distribution function is symmetric, and we interpret that as the indicator of commensurate contributions of short- and long-range interactions to the relaxation process. Simultaneously, the breadth of the distribution function increases with cure, analogous to the normalized dielectric loss in the frequency domain representation.

The second important question is whether the distribution function is thermodielectrically simple, i.e., if its shape is independent of temperature. We find that the distribution function is independent of temperature (i.e., thermodielectrically simple) until about 60% conversion. Above that conversion the distribution function undergoes a pronounced change, and we note a particularly strong temperature effect on the short relaxation time (high frequency) end of the spectrum. An increase in temperature results in an upward shift and a broadening of the distribution function. There is no doubt that the underlying reason for this behavior is related to the effect on dipole dynamics by the chemophysical changes on the molecular level in the network at that stage of cure which are accompanied by the emergence of hydrogen-bonded complexes in neat and solvent-containing formulations alike. We remind the reader that this effect on the dielectric a process in the vicinity of gel point is manifested in various ways, including an increase in the apparent activation energy, an increase of the half-width of the normalized loss peak, and an abrupt decrease in the power-law exponent "*n*" which describes the short-range interactions.

F. Fragility Plots. In this section we describe how the fragility or cooperativity plots (Angell[28] and Ngai[29]) can be used to relate the progress of chemical reaction in the solvent-containing formulations to the change in fragility or cooperativity of segmental motions during network formation. Fragility or cooperativity plots contain the most probable relaxation time as a function of normalized reciprocal temperature, expressed as T/T_g or $(T - T_g)/T_g$, where T_g is commonly taken to represent the temperature at which the relaxation time attains an arbitrary value. The plots provide a graphical interpretation of the rate of acceleration of cooperativity with decreasing temperature. The advancement of reactions in cross-linking systems affects the shape and position of the fragility curve as a result of the changes in (1) molecular architecture, which is altered by the increase in intermolecular dynamic constrains caused by the reduced mobility, and (2) dielectric architecture, which is continually altered during the reaction as a result of the change in the concentration and type of dielectrically active species. The effect of OTP concentration on cooperativity *prior to the onset of chemical reactions* is shown in Figure 15. A strong non-Arrhenius response that characterizes the neat formulation[4] changes to a near-Arrhenius response in all solvent-containing formulations. An increase in the concentration of OTP is accompanied by a small but systematic increase in the steepness of the cooperativity plot.

We next constructed cooperativity plots for a number of formulations *during cure* (i.e., at various stages of network formation); an example is shown in Figure 16 for a 50/50 formulation. The initial *decrease* in the apparent activation energy and the steepness of the cooperativity plot reflect a continuing weakening of the intermolecular interactions between the segments containing epoxy group. This is a direct result of the replacement of epoxy groups (dominant contributors to the α process) during reaction with the less dielectrically active secondary and tertiary amines and the hydroxyl groups. This trend persists to about 55% conversion, at which point the emerging hydrogen-bonded complexes begin to increase the steric hindrance and intermolecular rigidity of the network, leading, in turn, to the creation of a higher energy state that is manifested by an *increase* in the apparent activation energy and the steepness of the cooperativity plot. With further cure, the hydrogen-bonded complexes begin to break up and the dipole dilution effect becomes the dominant force again, causing a rapid decrease in the slope. In the solvent-containing formulation, however, the steepness of the fragility plot in the later stage of cure is significantly higher than in the neat system. We reiterate that the observed changes in cooperativity are consistent with the trend in the activation energy described in Figure 9a,b, which is expected since both parameters describe the same underlying physical phenomenon.

Conclusions

We have examined the effect of a nonreactive, nonpolar solvent (*o*-terphenyl or OTP) on the reorientational dynamics of dipoles in a multifunctional epoxy−amine system during network formation. The presence of OTP

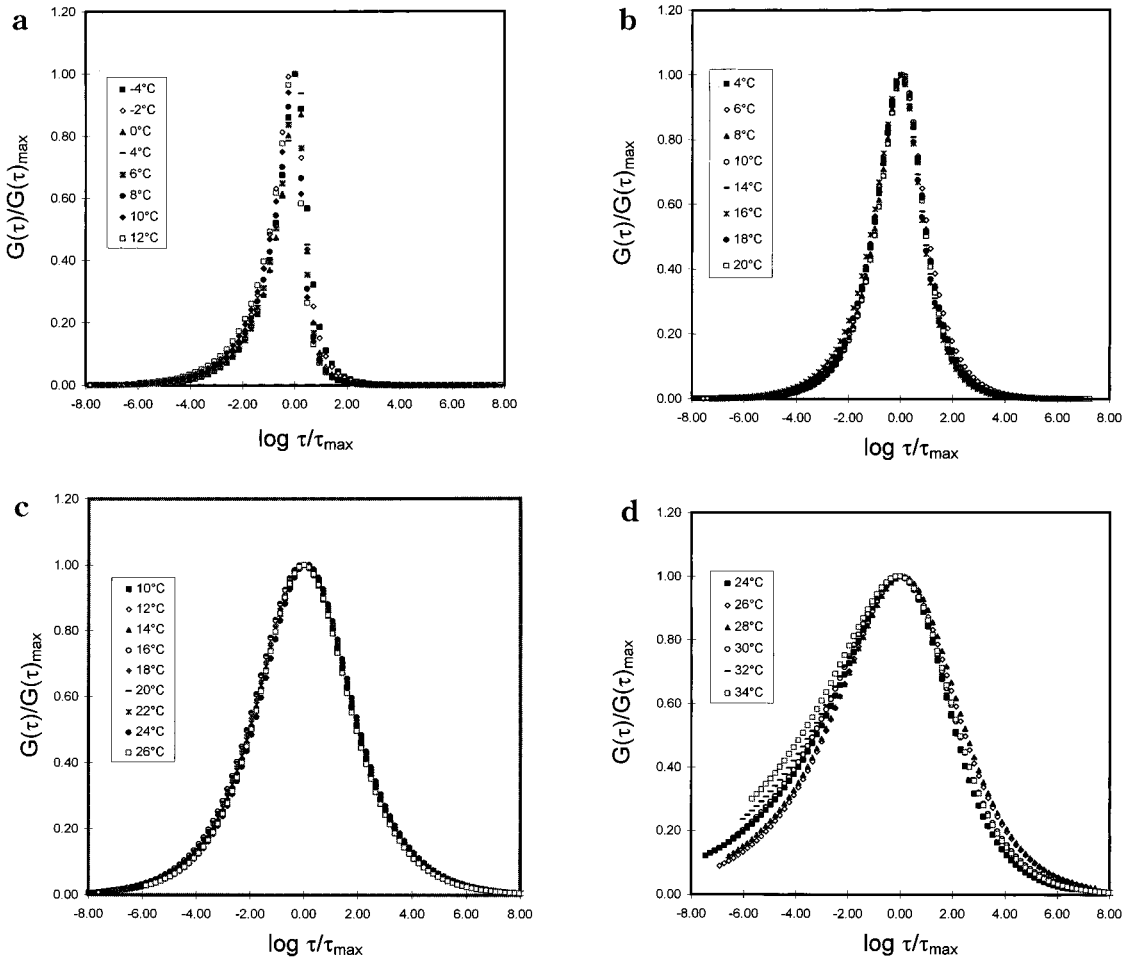

Figure 14. (a) Normalized distribution function as a function of normalized relaxation time for a 50/50 formulation cured to 10% conversion. (b) Same as part a for 33% conversion. (c) Same as part a for 55% conversion. (d) Same as part a for 60% conversion.

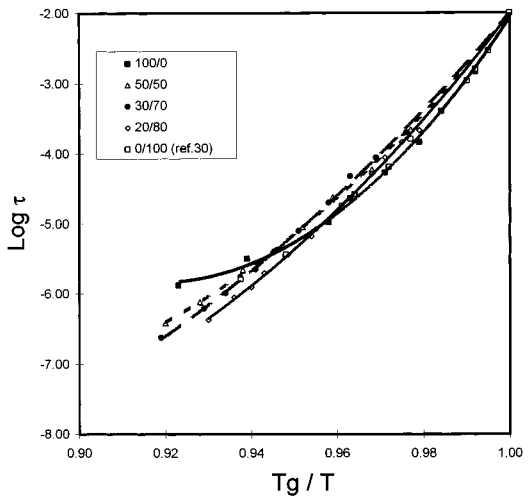

Figure 15. Cooperativity plot of relaxation time as a function of reduced temperature for OTP and a series of nonreacted formulations.

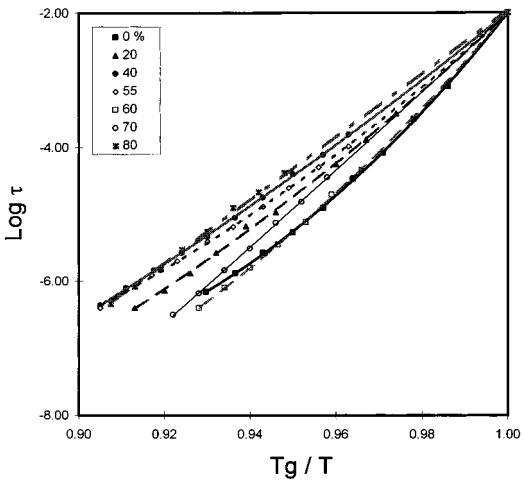

Figure 16. Cooperativity plot of relaxation time as a function of reduced temperature for 50/50 formulations at various stages during cure.

caused a decrease in the reaction rate but did not affect the reaction mechanism or interfere with the formation of hydrogen bonded complexes that accompanied gelation in this system. The solvent molecules influence dipole dynamics principally by increasing the distance between dipoles and introducing local strains that impede the relaxation process. Our major findings are recapped as follows.

(1) Dielectric and NIR data showed a significant decrease in dipolar interactions in the initial mixture with increasing concentration of solvent.

(2) A higher activation energy of the α-process compared to that of the neat system was observed in the later stages of cure.

(3) A pronounced broadening of the normalized relaxation peak was noted during cure.

(4) Normalized spectra in the frequency and time domain become symmetric during cure of solvent-

containing formulations, and no fits to KWW expression were possible above 10% conversion.

(5) Power law exponents "*m*" and "*n*", which are indicative of the longe-range and short-range motions, respectively, are useful indicators of the structural changes in the growing network.

(6) The distribution function becomes increasingly thermodielectrically complex above 60%.

Acknowledgment. This material is based on work supported by the National Science Foundation under Grant No. DMR-9710480.

References and Notes

(1) Fournier, J.; Williams, G.; Duch, C.; Aldridge, G. A. *Macromolecules* **1996**, *29*, 7097.
(2) Casalini, R.; Livi, A.; Rolla, P. A.; Levita, G.; Fioretto, D. *Phys. Rev. B* **1996**, *53*, 564.
(3) Casalini, R.; Fioretto, D.; Livi, A.; Lucchesi M.; Rolla, P. A. *Phys. Rev. B* **1997**, in press.
(4) Andjelic, S.; Fitz, B.; Mijovic, J. *Macromolecules* **1997**, *30*, 5239.
(5) Fitz, B.; Andjelic, S.; Mijovic, J. *Macromolecules* **1997**, *30*, 5227.
(6) Williams, G. In *Dielectric Spectroscopy of Polymeric Materials*; Runt, J. P., Fitzgerald J. J., Eds.; American Chemical Society: Washington, DC, 1997; Chapter 1, pp 3−65.
(7) Böttcher, C. J. F.; Bordewijk, P. *Theory of Electric Polarization*; Elsevier Scientific: Amsterdam, 1978.
(8) Williams, G.; Hains, P. J. *Chem. Phys. Lett.* **1971**, *10*, 585.
(9) Shears, M. F.; Williams, C. *J. Chem. Soc., Faraday Trans. 2* **1973**, *65*, 1050.
(10) Williams, G.; Shears, M. F. *J. Chem. Soc., Faraday Trans. 2* **1973**, *69*, 608.
(11) Williams, G.; Shears, M. F. *J. Chem. Soc., Faraday Trans. 2* **1973**, *69*, 1050.
(12) Matsuoka, S. *Relaxation Phenomena in Polymers*; Hanser: Munich, 1992.
(13) Donth E. J. *Relaxation and Thermodynamics in Polymers*; Akademie Verlag: Berlin, 1992.
(14) Kivelson, S. A.; Kivelson, D.; Zhao X.-L.; Nussimov, Z.; Tarjus, G. *Physica A* **1995**, *219*, 27.
(15) McLaughilin, E.; Ubbelohde, A. R. *Trans. Faraday Soc.* **1958**, *54*, 1804.
(16) Higashigaki, Y.; Wang, C. H. *J. Chem. Phys.* **1981**, *74*, 3175.
(17) Cicerone, M. T.; Ediger, M. D. *J. Chem. Phys.* **1996**, *104*, 7210.
(18) Mijovic, J.; Andjelic, S. *Macromolecules* **1995**, *28*, 2789.
(19) Mijovic, J.; Andjelic, S. *Polymer* **1995**, *36*, 3783.
(20) Mijovic, J.; Andjelic, S. *Polymer* **1996**, *37*, 1295.
(21) Mijovic, J.; Andjelic, S.; Yee, C. F. W.; Bellucci, F.; Nicolais, L. *Macromolecules* **1995**, *28*, 2797.
(22) Mijovic, J.; Fishbain, A.; Wijaya, J. *Macromolecules* **1992**, *25*, 979.
(23) Williams, G.; Watts, D. C. *Trans. Faraday. Soc.* **1970**, *66*, 80.
(24) Jonscher, A. K. *Dielectric Relaxation in Solids*; Chelsea Dielectric Press: London, 1983.
(25) Dissado, L. A.; Hill, R. M. *Nature* **1979**, *279*, 685.
(26) Schönhals, A.; Schlösser, E. *Colloid Polym. Sci.* **1989**, *267*, 125.
(27) Havrilliak, S.; Negami, S. *Polymer* **1967**, *8*, 161.
(28) Angell, C. A. *J. Non-Cryst. Solids* **1991**, *131−3*, 13.
(29) For a recent review, see: Ngai, K. L.; Plazek, D. J. *Rubber Chem. Technol.* **1996**, *68*, 376.
(30) Johari, G. P.; Smyth, C. P. *J. Chem. Phys.* **1972**, *56*, 4411.

MA9718513